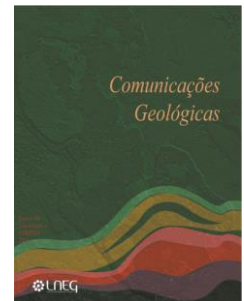


# Crustal stretching process denounced by mafic magmatism in the Finisterra Terrane; the yield of a back-arc basin?

## Processos de estiramento crustal evidenciados pelo magmatismo máfico do Terreno Finisterra; instalação de uma bacia de back-arc?



N. Moreira<sup>1\*</sup>, F. Noronha<sup>2</sup>, J. Pedro<sup>1</sup>, J. Romão<sup>3</sup>, R. Dias<sup>1</sup>, M. Sousa<sup>2</sup>, A. Ribeiro<sup>4</sup>, J. Roseiro<sup>1</sup>

Recebido em 14/11/2019 / Aceite em 18/12/2019

Publicado online em julho de 2020

© 2020 LNEG – Laboratório Nacional de Energia e Geologia IP

Artigo original  
Original article

**Abstract:** The occurrence of a new tectono-stratigraphic terrane (Finisterra Terrane), located in the westernmost domains of the Porto-Tomar-Ferreira do Alentejo Shear Zone, has been highlighted in the last few years. Nevertheless, there are several gaps in the geological knowledge of this Terrane, including the interpretation of existing data in the framework of the new tectono-stratigraphic terrane proposal, with an independent evolution from the Iberian Terrane. This work is an approach to the mafic magmatism significance that is described in the tectono-stratigraphic units from Abrantes-Tomar and Porto-Espinho-Albergaria-a-Velha sectors of the Finisterra Terrane. The geochemical data of the amphibolite rocks show affinities with mafic and ultramafic protholites with geochemical features between within-plate basalts and MORB. These amphibolites express specific geochemical features (*e.g.* N-MORB normalized Ba and Th enrichments, as well as Nb and Ta anomalies), suggesting their emplacement in a back-arc basin tectonic setting.

**Keywords:** Finisterra Terrane, mafic magmatism, geochemistry, crustal stretching, back-arc basin magmatism.

**Resumo:** A ocorrência de um terreno tectono-estratigráfico (Terreno Finisterra) localizado a Oeste da Zona de Cisalhamento Porto-Tomar-Ferreira do Alentejo tem sido posto em evidência ao longo dos últimos anos. Apesar dos trabalhos realizados no Terreno Finisterra, são várias as lacunas no conhecimento geológico deste terreno, bem como na interpretação dos dados existentes à luz da proposta de um novo terreno tectono-estratigráfico. No presente trabalho aborda-se a natureza do magmatismo máfico que ocorre nas unidades tectono-estratigráficas definidas para os diferentes setores do Terreno Finisterra, nomeadamente nos sectores de Abrantes-Tomar e Porto-Espinho-Albergaria-a-Velha. Os dados geoquímicos das rochas anfíbolíticas mostram a sua natureza máfica e ultramáfica, com assinaturas geoquímicas entre basaltos do tipo intraplaca a MORB. Estas rochas anfíbolíticas revelam características geoquímicas em elementos incompatíveis (*e.g.* incrementos em Ba e Th, assim como anomalias em Nb e Ta quando normalizados ao N-MORB), sugerindo a instalação em contexto tectónico do tipo bacia de back arc.

**Palavras-chave:** Terreno Finisterra, magmatismo máfico, geoquímica, estiramento crustal, bacia de back-arc.

<sup>1</sup>Instituto Dom Luiz, Dep. Geologia da Faculdade de Ciências da UL, Museu Nacional de História Natural e da Ciência (UL), Edifício C6, Piso 4, Campo Grande, 1749-016 Lisboa, Portugal.

\*Autor correspondente/Corresponding author:  
nmoreira@estremoz.cienciaviva.pt

### 1. Introduction

Basalt geochemistry is largely used in regional geological studies to recognize the emplacement setting and nature of the magmatic sources. Tracing the behavior of major and trace geochemical elements during tectonic processes was the subject of many statistical studies (*e.g.* Vermeesch, 2006; Pearce, 2014) that provided several trustworthy immobile element proxies (as they do not tend to mobilize during geological processes) and discrimination diagrams based on their relationships (decouple of geochemical pairs and enrichment-depletion rates due to metamorphic or alteration events; *e.g.* Pearce and Cann, 1973; Pearce, 1982; Pearce and Stern, 2006). These geochemical proxies and discrimination diagrams are important tools to fingerprint the tectono-magmatic environment associated with basalt genesis and evolution (*e.g.* Pearce and Cann, 1973; Pearce, 1982; Meschede, 1986; Pearce and Stern, 2006). The application and interpretation of these discrimination diagrams allow, in many cases, to discriminate the plate-tectonic setting and magma type of those mafic rocks. Nonetheless, in some cases, the discrimination of the tectono-magmatic environment is challenging, and, it is recommended to consider the isotopic data, whenever possible (*e.g.* Meschede, 1986; Pearce and Stern, 2006).

The geochemical discrimination of the tectono-magmatic environment of mafic rocks in highly metamorphosed and deformed domains is even more significant, as their primary petrographic features and the geological context are often obliterated, whereas the application of geochemical indicators with conservative/immobile behavior during metamorphism and/or weathering events remains valid (*e.g.* Pearce, 1982). Likewise, the study of these geochemical variations can be used as reliable indicators of petrogenesis and reflects the primary igneous features and processes involved in basalt geochemistry and geodynamical evolution.

Recent works in the Iberian Variscides proposed a new tectono-stratigraphic terrane located on the western domains of

<sup>1</sup>Instituto de Ciências da Terra (ICT), Pólo da Universidade de Évora; Departamento de Geociências da Escola de Ciências e Tecnologia da Univ. de Évora, Rua Romão Ramalho, nº 59, 7000-671 Évora, Portugal.

<sup>2</sup>Instituto de Ciências da Terra (ICT), Pólo da Universidade do Porto, Departamento de Geociências, Ambiente e Ordenamento do Território, Faculdade de Ciências da Univ. do Porto, Rua Campo Alegre, 4169-007 Porto, Portugal.

<sup>3</sup>UGHCG, Laboratório Nacional de Energia e Geologia, Estrada da Portela, Apartado 7586 - Zambujal, 2720 Alfragide, Portugal.

the Iberian Massif, the Finisterra Terrane (Ribeiro *et al.*, 2007, 2013a; Romão *et al.*, 2013, 2014; Moreira *et al.*, 2016, 2019a), East bounded by the Porto-Tomar-Ferreira do Alentejo Shear Zone (PTFSZ) (Fig. 1). In the tectonostratigraphic units of Finisterra Terrane, were reported (ultra)mafic ortho-derived rocks. Some of those rocks were studied (Montenegro de Andrade, 1977; Mendes, 1988; Chaminé, 2000; Noronha and Leterrier, 2000; Silva, 2007; Aires and Noronha, 2010), however the geodynamic significance of this magmatism is still debatable and the data were not interpreted considering the existence of a new tectonostratigraphic terrane.

This paper presents the first geochemical data of amphibolites from the Abrantes-Tomar sector, confronting with published data and discussing the meaning of the (ultra)mafic rocks of the Finisterra Terrane, accordingly to new proposed models (*e.g.* Ribeiro *et al.*, 2013a; Moreira *et al.*, 2019a).

## 2. Geological framework and previous works

The Finisterra Terrane is a newly proposed tectono-stratigraphic terrane of the Iberian Massif (Ribeiro *et al.*, 2007, 2013a; Romão *et al.*, 2013, 2014; Moreira *et al.*, 2016, 2019a), although the geodynamic significance of this terrane is still misunderstood, as well as its boundaries. The PTFSZ demarked the East boundary of Finisterra Terrane, defining its contact with two distinct paleogeographic and tectonic zones of the Iberian Terrane: Central Iberian and Ossa-Morena Zones (Romão *et al.*, 2013, 2014; Moreira *et al.*, 2019a). Although several authors (*e.g.* Dias and Ribeiro, 1993; Ribeiro *et al.*, 2007; Moreira *et al.*, 2019a) consider the PTFSZ a cryptic structure active, at least, during early Variscan times, others (*e.g.* Pereira *et al.*, 2010; Gutiérrez-Alonso *et al.*, 2015; Díez Fernandez and Pereira, 2017) consider that this shear zone was only active during Carboniferous times and interpret the PTFSZ as a large-scale high-strain transcurrent fault.

The western boundary of the Finisterra Terrane is hidden beneath the Lusitanian Basin, and is likely to represent a Variscan Oceanic suture (Rheic and/or Rheno-Hercynian Suture?) (Ribeiro *et al.*, 2007; Moreira *et al.*, 2019a). Although the geodynamic significance and evolution of the Finisterra Terrane is not consensual (*e.g.* Pereira *et al.*, 2010; Gutiérrez-Alonso *et al.*, 2015, 2016), the metamorphic, magmatic and tectono-stratigraphic features of this terrane seem to indicate an independent evolution between Finisterra and Iberian Terranes during the early stages of the Variscan Cycle (Moreira *et al.*, 2019a for discussion).

Along the Finisterra Terrane, three sectors, comprising several tectono-stratigraphic units with distinctive stratigraphic, structural, magmatic and metamorphic features, were defined (Moreira *et al.*, 2019a and references therein), being distinct from Iberian Terrane units.

The sectors along the Finisterra Terrane are, from North to South: (1) Porto-Espinho-Albergaria-a-Velha, (2) Coimbra and (3) Abrantes-Tomar. In the Porto-Espinho-Albergaria-a-Velha sector, four units are defined (Fig. 1B; Chaminé, 2000; Chaminé *et al.*, 2003):

- the Espinho and Lourosa Units (the Foz do Douro Metamorphic Complex, including Foz do Douro Gneiss Unit, is considered as equivalent of Lourosa Unit; Chaminé *et al.*, 2003) are high-grade para-derived metamorphic units, composed of micaschists and gneiss-migmatites, respectively. The Lourosa and Foz do Douro Gneiss Units include biotite orthogneisses with similar ages (ca. 450-420 Ma; Chaminé *et al.*, 1998; Sousa *et al.*, 2014);

- the Arada and Albergaria Units comprise medium to low-grade para-derived metamorphic units (biotite zone or less), both imbricated during the Variscan Orogeny.

Similar medium to low-grade para-derived metamorphic lithotypes were described in the Coimbra sector (Chaminé *et al.*, 2003; Ferreira *et al.*, 2007; Machado *et al.*, 2011). In the Abrantes-Tomar sector, only high-grade metamorphic units were described (Romão *et al.*, 2013; Moreira *et al.*, 2016, 2019a): the Junceira-Tramagal Micaschist Unit and the S. Pedro de Tomar Gneiss-Migmatitic Complex.

In some of these units occurs (ultra)mafic rocks, namely in the Arada, Lourosa, Foz do Douro Gneiss (Porto-Espinho-Albergaria-a-Velha sector; Fig. 1B) and the Junceira-Tramagal Units (Abrantes-Tomar sector; Fig. 1B). Geochemical features of the mafic rocks from the Porto-Espinho-Albergaria-a-Velha sector were studied (Montenegro de Andrade, 1977; Mendes, 1988; Chaminé, 2000; Noronha and Leterrier, 2000; Silva, 2007; Aires and Noronha, 2010), inferring their MORB to within-plate geochemical affinities. The age of these rocks is debatable:

- Noronha and Leterrier (2000) point a Neoproterozoic (1.05Ga) Sm-Nd model age for the amphibolites, with MORB geochemical affinities, from Foz do Douro Gneiss Unit. The authors suggested that this age should be similar with the mafic magmatism emplacement age;
- Almeida *et al.* (2014) obtained a middle to early Devonian age (391.9±1.6 Ma; U-Pb, LA-ICP-MS in zircons) for the olivine amphibolites from the Lourosa Unit. However, older concordant ages were obtained in these rocks (ca. 420-430 Ma; Moreira *et al.*, 2019a).

In the Coimbra and Abrantes-Tomar sectors, there are no geochemical studies of the mafic rocks: in the Coimbra sector (Arada Unit) the mafic dikes present high meteoric and metasomatic alteration degree (Ferreira *et al.*, 2007) and in the Abrantes-Tomar sector (Junceira-Tramagal Unit) only recently amphibolites dykes were reported (Moreira, 2017).

## 3. Sampling and methods

Three amphibolite samples were collected, two representing Junceira-Tramagal Unit (Abrantes-Tomar sector) and one from the Foz do Douro Gneiss Unit (Porto-Espinho-Albergaria-a-Velha sector).

Major and trace elements were analysed at the Activation Laboratories - ACTLABS (Canada) using the lithium metaborate/tetraborate fusion for ICP-OES (WRA Code 4B) and ICP-MS (WRA Code 4B2) - 4Lithoresearch analytical package, followed by 5% nitric acid digestion. Calibration was performed using seven USGS and Canmet certified reference materials. One of the seven standards is used during the analysis for every group of samples. The sample solution prepared under Code 4B is spiked with internal standards to cover the entire mass range. Analytical precision and accuracy for major elements are 1 to 2% and better than 5% for trace elements. Whole-rock geochemical data are summarized in table 1. New data were assembled and compared with published one (Montenegro de Andrade, 1977; Chaminé, 2000; Noronha and Leterrier, 2000; Silva, 2007; Aires and Noronha, 2010). Silva (2007) re-evaluated whole rock geochemistry data from Mendes (1988), and thus the geochemical data from the latter author (obtained with X-ray fluorescence spectrometry) was not used in this work.

## 4. Finisterra Terrane amphibolites: geochemical data

In the Junceira-Tramagal Unit, amphibolites (hornblende + plagioclase + opaque phases ± quartz) correspond to basalts with

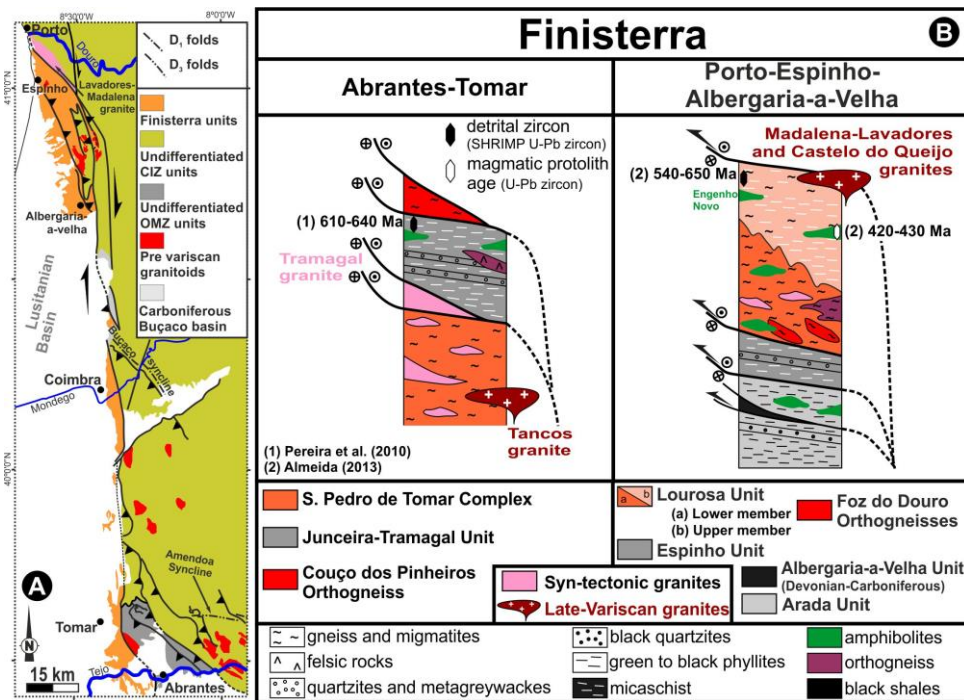


Figure 1. (A) Simplified geological map of the Finisterra Terrane and (B) the tectono-stratigraphy of the Abrantes-Tomar and Porto-Espinho-Albergaria-a-Velha sectors (adapted from Moreira *et al.*, 2019).

Figura 1. (A) Mapa geológico simplificado do Terreno Finisterra e (B) organização tectono-estratigráfica dos sectores de Abrantes-Tomar e Porto-Espinho-Albergaria-a-Velha (adaptado de Moreira *et al.*, 2019).

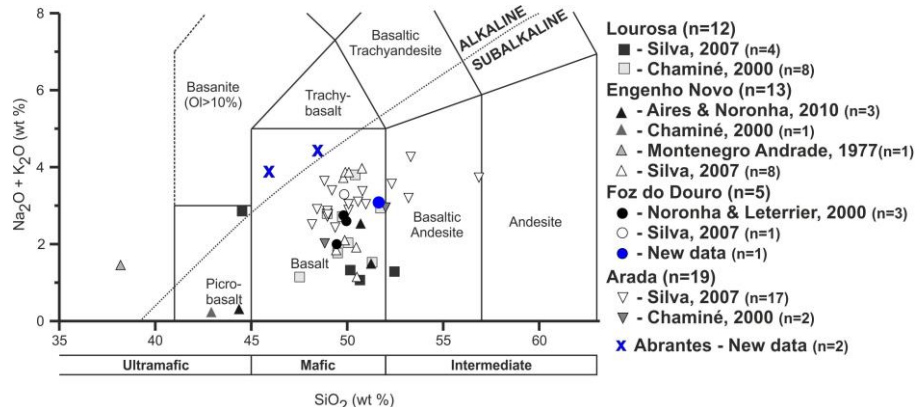


Figure 2. Total Alkalies vs. silica diagram for Finisterra Terrane amphibolite rocks (adapted from Le Maitre *et al.*, 1989; alkaline-subalkaline curve from Irvine and Baragar, 1971).

Figura 2. Diagrama Alcalis total vs. sílica para as rochas anfíbolíticas do Terreno Finisterra (adaptado de Le Maitre *et al.*, 1989; curva de divisão entre série alcalina-subalcalina de Irvine e Baragar, 1971).

transitional alkaline-subalkaline features ( $\text{SiO}_2 = 45.97\text{-}48.49$  wt.%;  $\text{CaO} = 9.14\text{-}10.75$  wt.%;  $\text{Na}_2\text{O} + \text{K}_2\text{O} = 3.89\text{-}4.52$  wt.%;  $\#\text{Mg} = 29.14\text{-}29.68$ ) (Fig. 2 and Tab. 1).

In the Lourosa and Foz do Douro Gneiss Unit, (garnet-) amphibolites (hornblende + plagioclase + opaque phases + sphene  $\pm$  garnet  $\pm$  epidote  $\pm$  quartz) correspond to subalkaline basalts and basaltic andesites ( $\text{SiO}_2 = 47.54\text{-}56.89$  wt.%;  $\text{Na}_2\text{O} + \text{K}_2\text{O} = 1.05\text{-}3.78$  wt.%;  $\text{CaO} = 8.17\text{-}12.82$  wt.%;  $\#\text{Mg} = 31.07\text{-}55.35$ ), or rarely transitional picro-basalts ( $\text{SiO}_2 = 44.54$  wt.%;  $\text{Na}_2\text{O} + \text{K}_2\text{O} = 2.81$  wt.%;  $\text{CaO} = 12.19$  wt.%;  $\#\text{Mg} = 36.73$ ) (Fig. 2) (Mendes, 1988; Noronha and Leterrier, 2000; Silva, 2007). In the Engenho Novo locality (Lourosa Unit), beyond the metabasaltic rocks, an olivine amphibolite (primary olivine [and serpentine] + amphibole + chlorite + opaque phases) with ultramafic affinity ( $\text{SiO}_2 = 38.22\text{-}44.35$  wt.%;  $\text{Na}_2\text{O} + \text{K}_2\text{O} = 0.19\text{-}1.45$  wt.%;  $\text{CaO} = 3.19\text{-}5.02$  wt.%;  $\#\text{Mg} = 73.93\text{-}88.14$ )

were reported (Montenegro de Andrade, 1977; Chaminé, 2000; Aires and Noronha, 2010).

In the Arada Unit, amphibolites and amphibolic schists (amphibole + plagioclase + quartz + opaque phases + epidote + sphene  $\pm$  chlorite  $\pm$  biotite) correspond to subalkaline basalts and basaltic andesites ( $\text{SiO}_2 = 48.15\text{-}56.89$  wt.%;  $\text{Na}_2\text{O} + \text{K}_2\text{O} = 2.00\text{-}4.27$  wt.%;  $\text{CaO} = 6.94\text{-}11.53$  wt.%;  $\#\text{Mg} = 26.92\text{-}59.75$ ) (Fig. 2), recording an amphibolite to epidote-amphibole metamorphic facies conditions (Mendes, 1988; Silva, 2007).

#### 4.1. Junceira-Tramagal amphibolites

Both amphibolite samples show similar patterns with considerable enrichment in Rare Earth Elements (REE) content relative to the C1 chondrite (Tab. 2 and Fig. 3A), high fractionation of LREE over MREE and HREE, and do not display Eu and Ce anomalies (Tab. 2 and Fig. 3A). The REE

patterns are comparable with global Continental Volcanic Arc Andesites and OIB patterns (Fig. 3A; Sun and McDonough, 1989; Kelemen *et al.*, 2014). These amphibolite samples are enriched in Ti ( $[2.4] \times \text{N-MORB}$ ) and have high contents in Th ( $[12.4-12.5] \times \text{N-MORB}$ ), Ba ( $[12.4-12.5] \times \text{N-MORB}$ ), Nb ( $[6.7-7.2] \times \text{N-MORB}$ ), Ta ( $[8.41-8.48] \times \text{N-MORB}$ ), La ( $[6.60-7.04] \times \text{N-MORB}$ ) and Sr ( $[12.4-12.5] \times \text{N-MORB}$ ).

## 4.2. Foz do Douro Amphibolites

The C1 chondrite normalized REE contents from Foz do Douro amphibolites show two groups with similar patterns:

(G1) Three amphibolites (including the new analyzed sample; Fig. 3B) present considerable enrichment of REE content relatively to the C1 chondrite, with significant depletion of LREE relatively to MREE and HREE and do not present Eu and Ce anomalies, showing a REE pattern similar to those characterizing the N-MORB (Tab. 2 and Fig. 3B; Sun and McDonough, 1989). These amphibolites present similar Ti ( $[1.00-1.43] \times \text{N-MORB}$ ), Ta ( $[1.29] \times \text{N-MORB}$ ) and La ( $[0.89-1.87] \times \text{N-MORB}$ ) contents to N-MORB, showing some variability in Nb content ( $[0.33-1.82] \times \text{N-MORB}$ ) and being slightly enriched in Th ( $[2.42] \times \text{N-MORB}$ ) and Ba ( $[2.68-3.56] \times \text{N-MORB}$ ).

(G2) Two amphibolites are enriched of REE content relatively to the C1 chondrite, with LREE similar to MREE and HREE and without Eu and Ce anomalies, displaying a REE pattern intermediate between the N-MORB and E-MORB typical patterns (Tab. 2 and Fig. 3B; Sun and McDonough, 1989). These amphibolites do not show significant variations in Ti contents in relation to N-MORB ( $[1.13-1.28] \times \text{N-MORB}$ ), and are slightly enriched in Ta ( $[2.35] \times \text{N-MORB}$ ), La ( $[1.82-2.02] \times \text{N-MORB}$ ), Nb ( $[2.01-2.49] \times \text{N-MORB}$ ), Th ( $[3.83] \times \text{N-MORB}$ ) and Ba ( $[3.17-3.29] \times \text{N-MORB}$ ).

## 4.3. Lourosa Amphibolites

The Lourosa Unit includes two distinct lithotypes: olivine amphibolites and amphibolites. The olivine amphibolites (n=3) are enriched in REE content relatively to the C1 chondrite (Tab. 2 and Fig. 3C), with slightly enrichment in LREE over MREE and HREE, and negative Eu and Ce anomalies. The olivine amphibolite samples are generally depleted in HSE and REE relatively to N-MORB, with low Ti ( $[0.37-0.85] \times \text{N-MORB}$ ), Zr ( $[0.27-0.44] \times \text{N-MORB}$ ) and Nb ( $[0.34] \times \text{N-MORB}$ ), similar Th ( $[1.25] \times \text{N-MORB}$ ) and La ( $[1.03] \times \text{N-MORB}$ ) and high Cr and Ni (Cr = 1660-2080 ppm; Ni = 840-1000 ppm) contents.

The C1 chondrite normalized REE content and ratios from Lourosa amphibolites (including the Engenho Novo amphibolites without olivine) show two distinct patterns:

(G2) Amphibolites (n=11) with considerable enrichment of REE content relatively to the C1 chondrite, with LREE similar to MREE and HREE, and do not present Eu and Ce anomalies, with exception of one amphibolite that presents marked negative Ce anomaly (Ce/Ce\* 0.54). Normalized REE contents of these mafic rocks are intermediate to the N-MORB and E-MORB patterns (Fig. 3C; Sun and McDonough, 1989). These amphibolites displays slightly high Ti ( $[1.10-2.42] \times \text{N-MORB}$ ) and Nb ( $[1.50-5.06] \times \text{N-MORB}$ ) contents, and are enriched in Th ( $[2.17-7.83] \times \text{N-MORB}$ ), Ba ( $[5.40-16.51] \times \text{N-MORB}$ ), Ta ( $[1.74-4.92] \times \text{N-MORB}$ ) and La ( $[2.05-4.62] \times \text{N-MORB}$ ). The amphibolite with negative Ce anomaly exhibits anomalous Ba ( $[16.83] \times \text{N-MORB}$ ) content and high La/Ta ratio (41.79).

(G3) Amphibolites (n=3) present considerable enrichments in REE content relatively to the C1 chondrite, denoting

significant fractionation of LREE over MREE and HREE, with a REE pattern similar to those characterizing the E-MORB (Fig. 3C; Sun and McDonough, 1989), and do not show significant Eu and Ce anomalies (Tab. 2). These amphibolites present high Ti content ( $[2.04-3.05] \times \text{N-MORB}$ )

Table 1. Major (%) and trace (ppm) element analyses of amphibolites from Finisterra Terrane.

Tabela 1. Análises de elementos maiores (%) e traço (ppm) de amphibolitos do Terreno Finisterra.

	Junceira-Tramagal Micaschist Unit (Abrantes)		Foz do Douro Gneiss unit
	GQAB 12A	GQAB 12B	ANFGON01
	Amphibolite N39.44897 W8.22280	Amphibolite N39.44897 W8.22280	Amphibolite N41.15468 W8.68067
SiO <sub>2</sub>	45.81	48.07	49.47
Al <sub>2</sub> O <sub>3</sub>	18.44	18.13	14.31
Fe <sub>2</sub> O <sub>3</sub> (T)	13.05	12.12	10.59
MnO	0.17	0.16	0.18
MgO	4.20	3.80	8.19
CaO	10.71	9.06	8.48
Na <sub>2</sub> O	3.35	3.87	2.56
K <sub>2</sub> O	0.53	0.61	0.39
TiO <sub>2</sub>	3.06	2.97	1.49
P <sub>2</sub> O <sub>5</sub>	0.30	0.31	0.13
LOI	0.84	0.97	4.85
<b>TOTAL</b>	<b>100.5</b>	<b>100.1</b>	<b>100.6</b>
Sc	27	26	39
Be	1	1	< 1
V	368	353	322
Cr	40	30	290
Co	43	36	37
Ni	< 20	< 20	90
Cu	20	20	20
Zn	200	510	140
Ga	23	23	19
Ge	1.7	1.8	3.0
As	< 5	< 5	< 5
Rb	13	11	14
Sr	514	727	94
Y	19	20	33
Zr	126	129	96
Nb	15.5	16.7	2.8
Mo	< 2	< 2	< 2
Ag	< 0.5	< 0.5	0.60
In	< 0.1	0.10	< 0.1
Sn	1	2	5
Sb	0.3	< 0.2	0.4
Cs	4.70	0.50	0.80
Ba	159	261	22
La	18	17	4.3
Ce	39	38	12
Pr	4.94	4.91	2.02
Nd	22	21	10
Sm	5.04	4.97	3.72
Eu	1.63	1.82	1.29
Gd	5.10	4.89	4.55
Tb	0.69	0.75	0.84
Dy	3.99	4.14	5.80
Ho	0.68	0.74	1.17
Er	1.93	1.93	3.50
Tm	0.25	0.25	0.53
Yb	1.58	1.48	3.55
Lu	0.22	0.23	0.51
Hf	2.70	2.90	2.30
Ta	1.11	1.12	0.17
W	0.50	3.50	< 0.5
Ti	0.11	0.05	< 0.05
Pb	64	97	< 5
Bi	0.10	0.40	0.40
Th	1.49	1.50	0.29
U	0.53	0.54	0.31

and are highly enriched in Nb ( $[5.28-13.73] \times \text{N-MORB}$ ), Ta ( $[5.83-18.86] \times \text{N-MORB}$ ), La ( $[5.20-10.36] \times \text{N-MORB}$ ), Th ( $[8.08-26.42] \times \text{N-MORB}$ ) and Ba ( $[7.62-34.13] \times \text{N-MORB}$ ) in relation to N-MORB.

#### 4.4. Arada Amphibolites

In Arada Unit, both amphibolites and amphibolic schists show similar patterns. The C1 chondrite normalized REE contents and ratios allow to discriminate three groups:

- (G1) Amphibolites (n=6) with considerable enrichment of REE contents relatively to the C1 chondrite, significant depletion of LREE over MREE and HREE (REE pattern similar to those characterizing the N-MORB; Fig. 3D; Sun and McDonough, 1989), and without Eu and Ce anomalies, although one sample have a positive Eu anomaly ( $\text{Eu}/\text{Eu}^* 1.43$ ). These amphibolites present similar or lower Ti ( $[0.37-1.27] \times \text{N-MORB}$ ), Ta ( $[0.15-0.83] \times \text{N-MORB}$ ) and La ( $[0.26-1.18] \times \text{N-MORB}$ ) contents, high variability in Th content ( $[0.42-1.75] \times \text{N-MORB}$ ), low Nb ( $[0.52-0.94] \times \text{N-MORB}$ ) and Zr ( $[0.22-0.98] \times \text{N-MORB}$ ) and similar Ba ( $[1.27-3.33] \times \text{N-MORB}$ ) contents relatively to N-MORB.
- (G2) The amphibolites (n=7) are enriched in REE relatively to the C1 chondrite, showing flat REE patterns, intermediate between the N-MORB and E-MORB features (Tab. 2 and Fig 3D; Sun and McDonough, 1989). These amphibolites generally do not present Eu and Ce anomalies, although negative Ce anomaly was identified in two amphibolites ( $\text{Ce}/\text{Ce}^* 0.65-0.80$ ) and Eu negative anomaly in one ( $\text{Eu}/\text{Eu}^* 0.74$ ) (Fig. 3D). These amphibolites present slightly higher Ti ( $[1.21-2.19] \times \text{N-MORB}$ ), Ta ( $[2.05-4.02] \times \text{N-MORB}$ ), La ( $[2.60-4.64] \times \text{N-MORB}$ ) and Nb ( $[1.93-4.98] \times \text{N-MORB}$ ), and are enriched in Th ( $[3.33-9.42] \times \text{N-MORB}$ ) and Ba ( $[4.60-9.52] \times \text{N-MORB}$ ) contents. The amphibolites with

negative Ce anomaly present higher Ba content ( $[7.94-9.52] \times \text{N-MORB}$ ) when compared to other amphibolites ( $[4.60-7.46] \times \text{N-MORB}$ ), as well as high La/Ta ratios ( $37.04-42.96$ ).

- (G3) Amphibolites (n=4) present significant enrichment of REE content relatively to the C1 chondrite, with high fractionation of LREE over MREE and HREE, and present negative Eu and Ce anomalies, showing a REE pattern similar to those characterizing the E-MORB (Table 2 and Fig. 3D; Sun and McDonough, 1989). These amphibolites have high Ti contents ( $[1.20-2.38] \times \text{N-MORB}$ ), and are highly enriched in Nb ( $[3.43-4.72] \times \text{N-MORB}$ ), Th ( $[7.33-53.75] \times \text{N-MORB}$ ), Ta ( $[3.71-6.14] \times \text{N-MORB}$ ), La ( $[5.60-12.16] \times \text{N-MORB}$ ) and Ba ( $[4.92-12.92] \times \text{N-MORB}$ ).

#### 5. Geochemical significance of the Finisterra mafic magmatism

The Finisterra mafic rocks show heterogeneous geochemical features and the Porto-Espinho-Albergaria-a-Velha sector amphibolites (Foz do Douro, Lourosa and Arada) are clustered in three distinct groups. The G1 amphibolites have C1 chondrite normalized REE patterns very similar to N-MORB (Sun and McDonough, 1989), though with frequent enrichments in some incompatible elements, as Th and Ba (Fig. 3). The G2 and G3 amphibolites are REE enriched, with similarities to C1 chondrite normalised E-MORB pattern (Fig. 3), usually with higher content in some incompatible elements like Th, Ba, Nb, Ta or La. The G2 amphibolites display transitional features between the G1 and G3 groups. A quite distinctive feature of some G2 and G3 amphibolites is the recurrent negative Ce anomaly, with greater preponderance in the Lourosa and Arada units (Fig. 3C, D). The presence of this anomaly in both groups seems to indicate that the three groups could be related, tracing an evolutionary pattern.

Table 2. Main elemental relations (ranging minimum-maximum) of mafic ortho-derived rock groups of Finisterra Terrane Units (including data from this study and bibliographic data from: Montenegro de Andrade, 1977; Chaminé, 2000; Noronha and Leterrier, 2000; Silva, 2007; Aires and Noronha, 2010; N-MORB, E-MORB and OIB data from Sun and McDonough, 1989; Continental Volcanic Arc Andesites (CVA) from Kelemen *et al.*, 2014; and Ti/V range from Shervais, 1982).

Tabela 2. Principais relações elementares (intervalo de valores mínimo-máximo) para os grupos de rochas orto-derivadas de natureza máfica das Unidades do Terreno Finisterra (inclui novos dados e dados bibliográficos de: Montenegro de Andrade, 1977; Chaminé, 2000; Noronha e Leterrier, 2000; Silva, 2007; Aires e Noronha, 2010; dados de N-MORB, E-MORB e OIB retirados de Sun e McDonough, 1989; dados de Andesitos de Arco Vulcânico (CVA) baseados em Kelemen *et al.*, 2014; e intervalos de Ti/V de Shervais, 1982).

	Junceira-Tramagal Unit	Foz do Douro Gneiss Unit		Lourosa Unit			Arada Unit			N-MORB	E-MORB	OIB	CVA
		G1	G2	OL-Amp	G2	G3	G1	G2	G3				
La <sub>C1n</sub>	69.62 - 74.26	9.40 - 19.74	19.16 - 21.35	10.84	18.35 - 51.90	50.85 - 109.28	2.78 - 12.45	27.38 - 48.95	59.07 - 128.27	10.55	26.58	156.1 2	79.7 0
Sm <sub>C1n</sub>	32.48 - 32.94	18.69 - 27.78	22.68 - 24.97	8.36	18.76 - 51.24	40.52 - 74.51	6.60 - 24.71	29.80 - 44.71	31.50 - 64.84	17.19	16.99	65.36	25.6 2
Yb <sub>C1n</sub>	8.71 - 9.29	17.29 - 25.20	17.88 - 20.24	7.41	17.29 - 35.59	24.59 - 48.24	8.94 - 23.18	24.65 - 36.41	24.02 - 40.71	17.94	13.94	12.71	9.06
[La/Sm] <sub>C1n</sub>	2.14 - 2.25	0.50 - 0.75	0.84-0.96	1.30	0.75 - 1.10	1.35 - 1.68	0.42 - 0.62	0.76 - 1.30	1.41 - 2.54	0.61	1.56	2.39	3.11
[La/Yb] <sub>C1n</sub>	7.99 - 8.00	0.54 - 0.87	1.03-1.07	1.46	0.90 - 1.52	2.23 - 2.36	0.31 - 0.62	0.93 - 1.83	2.16 - 5.19	0.59	1.91	12.29	8.80
Eu/Eu*	0.97 - 1.12	0.92 - 1.10	0.99-1.03	0.63	0.93 - 1.20	0.93 - 1.03	0.89 - 1.43	0.74 - 1.05	0.76 - 0.95	1.00	1.00	1.01	0.83
Ce/Ce*	1.00 - 1.02	1.01 - 1.04	1.02-1.03	0.84	0.54 - 1.02	0.91 - 1.02	0.85 - 1.06	0.65 - 1.05	0.65 - 0.95	1.00	1.02	1.01	0.90
Ti/Zr	139.10 - 146.10	93.75 - 106.49	93.31 - 99.54	97.16 - 323.73	77.36 - 140.57	77.05 - 93.70	128.49 - 182.00	89.01 - 110.78	60.02 - 96.56	102.70	82.19	61.43	34.5 2
Ti/V	50.09 - 50.83	25.81 - 31.98	28.91 - 29.70	8.24 - 31.13	28.89 - 41.95	43.37 - 53.08	14.12 - 27.88	32.45 - 36.81	34.29 - 55.73	20-50	50-100	29.9 2	
Th/Ta	1.34	1.71	1.48	2.50	0.93 - 1.62	0.95 - 2.60	1.36 - 2.63	1.29 - 2.59	1.80 - 8.17	0.91	1.28	1.48	5.31
Ba/Nb	10.26 - 15.63	3.99 - 28.72	3.45 - 4.41	5.00	1.50 - 16.25	1.78 - 12.36	6.67 - 16.67	2.50 - 13.33	2.82 - 7.57	2.70	6.87	7.29	63.1 9
Nb/Ta	13.96 - 14.91	16.47	18.71	13.33	12.96 - 40.71	12.85 - 15.97	20.00 - 60.00	16.42 - 22.31	13.58 - 16.33	17.65	17.66	17.78	9.34
La/Ta	14.73 - 15.86	25.35	16.32	42.83	15.36 - 41.79	6.91 - 21.23	25.33 - 52.75	15.48 - 42.96	20.59 - 44.29	18.94	22.22	13.70	22.2 2

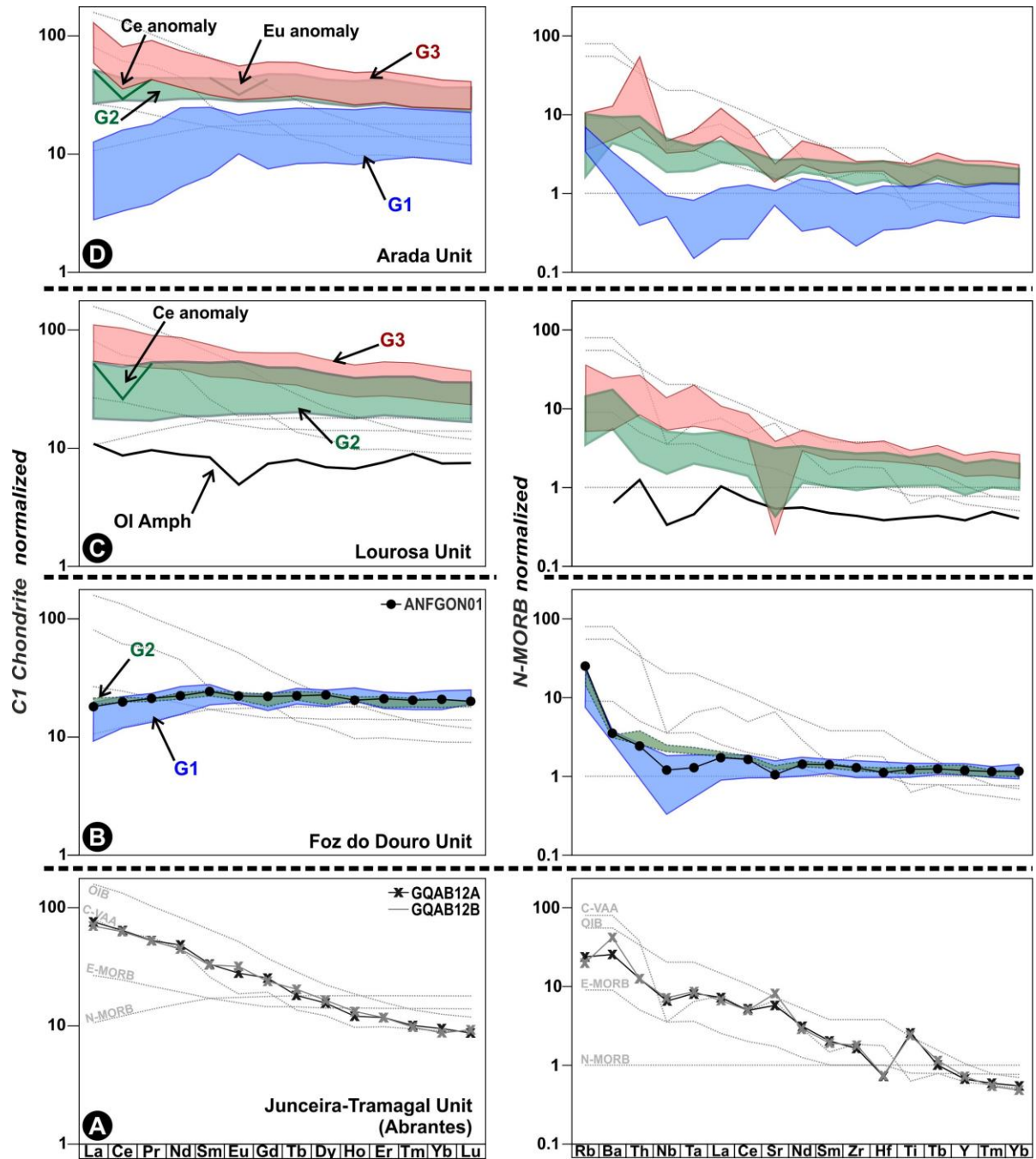


Figure 3. C1 Chondrite-normalized REE and N-MORB-normalized incompatible elements pattern diagrams from Finisterra Terrane ortho-derived amphibolites (C1 Chondrite and N-MORB values from Sun and McDonough, 1989).

Figura 3. Diagrama de padrões de Elementos Terras Raras normalizados ao Condrito C1 e de elementos incompatíveis normalizados ao N-MORB para as rochas anfibolíticas do Terreno Finisterra (valores de normalização ao Condrito C1 e N-MORB de Sun e McDonough, 1989).

The Abrantes-Tomar amphibolites (Junceira-Tramagal unit) are distinct, presenting alkaline-tholeiitic transitional features, with high fractionation of REE, coupled with an enrichment in incompatible trace elements like Ba, Th, Nb, Ta and even Sr (Fig. 3A). These amphibolites, although with significant differences, have some similarities with G3 group. Generally, G3 group is more depleted in Sr than the Abrantes amphibolites, although both are clearly enriched in Ba, Th, Ta and La relatively to N-MORB (Fig. 3). However, it should be noted that all these rocks record amphibolite facies metamorphic conditions (or epidote-amphibolite facies in the Arada Unit), and Sr is noticeably

affected by high grade metamorphism (Pearce and Cann, 1973), and thus its use as a proxy should be avoided. The immobility of Ba, Th, Nb and Ta during metamorphic and weathering events can be inferred using the methodology proposed by Cann (1970), which studied the behavior of each element according to their correlation with an immobile element, as Zr (validated by Pearce, 2014). This approach denotes that all these elements have a similar behavior and moderate to strong correlations with Zr. Nonetheless the high dispersion of Ba/Zr values, the main trend and moderate correlation (Fig. 4) assures Ba used as a proxy. Likewise, it is considered that all these elements express primary

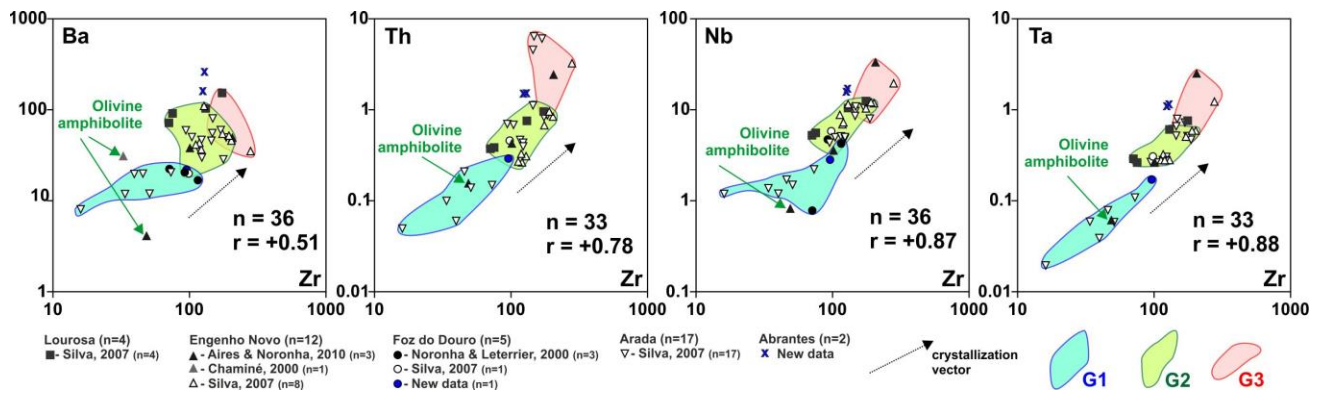


Figure 4. Cross plot diagrams of Ba, Th, Nb and Ta in relation to Zr, used for testing the immobile behavior of these elements (based on Cann, 1970 and Pearce, 2014).

Figura 4. Diagramas binários da relação do Ba, Th, Nb e Ta com o Zr, utilizado para testar o carácter imóvel destes elementos (baseados em Cann, 1970 e Pearce, 2014).

magmatic concentrations and thus can be used as discriminant proxies for geotectonic settings.

Therefore, assuming that the Finisterra amphibolite rocks are related with the same geodynamic event, they can be interpreted as a coeval event. The Ti-Zr ratios define a positive trend from the MORB and within-plate basalts fields (Fig. 5A). However, the Engenho Novo olivine amphibolites and G1 amphibolites from Arada unit are depleted in Zr and Ti and have similarities with volcanic arc basalts. The presence of olivine phenocrysts in mafic rocks reduce the absolute amounts of Ti, Zr, Y, Nb and Sr, and increase the MgO, Cr or Ni contents (Pearce and Cann, 1973), which can explain the projection of olivine amphibolites in the volcanic arc field (Fig. 5A), but not the G1 amphibolites (depleted in Zr and Ti relatively to N-MORB and enriched in Mg, but unaccompanied by Cr and Ni contents).

The three amphibolite groups from Porto-Espinho-Albergaria-a-Velha sector generally show Ti/V ratio similar to those characterizing the MORB to back-arc basin basalts (BABB) array, while the Abrantes-Tomar amphibolites show a quite higher Ti/V (Tab. 2), compatible with their alkali-tholeiitic transitional features (Shervais, 1982). Similar behavior is indicated in the Nb-Zr-Y diagram (Fig. 5B): the G1 and G2 amphibolites are both projected in the N-MORB – volcanic arc basalts (VAB) field, the G3 amphibolites between E-MORB and N-MORB–VAB field, and the Abrantes amphibolites indicate alkali-tholeiitic transitional within-plate features.

The Th-Ta diagram (Fig. 5C) permits a well discrimination of mafic magmatism, also suggesting the input of some elements, like Th, in the primary magma source. This diagrams clearly show the segregation of previous reported groups: (1) Abrantes amphibolites are projected in within-plate basalts field, with alkaline-tholeiitic transitional features; (2) the G1 and G2 amphibolites are projected over of MORB field, in the island arc tholeiites domain; and (3) the G3 amphibolites are projected over the tholeiitic within-plate to MORB domains, in the volcanic-arc calc-alkaline basalts field. All the G1, G2 and G3 amphibolites present Th/Ta higher than 1. The analysis of the presented diagrams seems to indicate that all mafic rocks are generated during a crustal stretching process, with generation of MORB and within plate basalts. The presented data is in agreement with Sm-Nd isotope data (Noronha and Letierrier, 2000), which indicate a mantellic source for Foz do Douro MORB-like amphibolites. The presence of high Th/Yb ratio in G1 to G3 amphibolites seems to indicate a Th input in the basaltic magmas, which agrees with the generalized enrichment of other incompatible elements, such as Ba, Nb, Ta and La, mainly in G2 and G3 groups. The amphibolite samples are generally depleted in Nb and Ta in comparison to other incompatible elements (Th

and La), as evidenced by the N-MORB normalized diagrams (Tab. 2 and Fig. 3). This enrichment of mantle derived mafic melts could be explained by two processes (Pearce, 1982; Pearce and Stern, 2006): (1) crustal assimilation during magma emplacement or (2) contamination during subduction and oceanic metasomatism of mantle magmas during subduction or arc-type volcanism, typical of the generation of a back-arc basin basalts.

The geochemical discrimination between MORB and BABB is quite challenging (Pearce and Cann, 1973; Pearce and Stern, 2006). According to Pearce and Stern (2006), BABB magmas can have MORB features and variable subduction components, generally showing transitional features between MORB and Island Arc Basalts (IAB; Fig. 5D); the BABB are generally enriched in subduction-mobile elements, such as Ba, Sr, La or Th, and depleted in subduction-immobile elements (Pearce and Stern, 2006). All the Finisterra amphibolites show significant enrichment in Ba and Th relatively to N-MORB (Figs. 3 and 5C), even the G1 amphibolites which presents the most primitive composition. The G2 and G3 amphibolites are generally enriched in La, Th and, to a lesser extent, in Ta and Nb (both showing N-MORB-normalized negative anomaly as respect to La and Th; Fig. 3 and Tab. 2), which is also in accordance with the typical N-MORB normalized LILE-HSFE pattern of BABB, emphasized by Pearce and Stern (2006). N-MORB depleted G1 amphibolites also show higher La and Th fractionation over Ta and Nb. In turn, the Abrantes amphibolites, although enriched in La and Sr, do not present the typical depletion of Nb and Ta, as respect to Th and La. The data projection on Ba-Nb diagram (Fig. 5D) shows that G1, G2 and G3 amphibolites do not present Ba/Nb ratios similar to volcanic-arc basalts and show a Ba enrichment regarding the typical MORB array (Tab. 2). The Engenho Novo olivine amphibolite presents similar behaviour to these amphibolites, which could denote a similar magmatic source, with high Ba content (presumably with input of subduction-derived components). The increase of Ba in G1 to G3 is also accompanied by Nb enrichment (Fig. 5D). The Abrantes amphibolites are projected in VAB field on Ba-Nb diagram (Fig. 5D), which is in accordance with high Ba/Nb comparatively to MORB-like rocks (Tab. 2), and with C1 chondrite and N-MORB normalized patterns quite similar to those that characterize the continental volcanic arc rocks (Fig. 3A). The possible BABB nature of some Finisterra amphibolites is also emphasized in Th-Ta diagram (Cabanis and Thiéblemont, 1988; Fig. 5E); most amphibolites are projected within MORB and BABB fields. This diagram also confirms the within-plate transitional features of the Abrantes amphibolites (Fig. 5E).

The negative Ce anomalies observed in C1 chondrite normalized REE from amphibolites of G2 and G3 can also be a

key feature to understand the evolution of these mafic magmas. This anomaly is commonly interpreted as the result of addition of subducted derived elements to the mantle magma sources (*e.g.* Hole *et al.* 1984; Shimizu *et al.*, 1992; Bellot *et al.*, 2018), being in accordance with the back-arc basin setting hypothesis for these mafic magmas. The negative Ce anomalies observed in chondrite-normalized REE from amphibolites of G2 and G3 could also be explained by assimilation of continental crust rocks by mafic magmas, namely metasedimentary rocks with Ce negative anomaly signature (*e.g.* reduced black shales; German and Elderfield, 1990; Shimizu *et al.*, 1992). The amphibolites with negative Ce anomaly always present anomalously higher Ba content, providing an evidence for relation between both features. The olivine amphibolite also present negative Ce anomaly (Fig. 3B), suggesting a similar petrogenetic evolution. Neal and Taylor (1989) reported similar behavior in peridotite xenoliths and presented a model of mantle mixing with subduction derived sources, considering three mixing members: mantle peridotite, sediment and seawater-altered basalt. Accordingly, two possible explanations are plausible for the generation of Engenho Novo ultramafic rocks: (1) olivine fractionation on mafic magma (as

proposed by Mendes, 1988), which already present negative Ce anomaly in the magmatic source, or (2) injection of ultramafic rocks on continental crust during the continental stretching process (as proposed by Chaminié, 2000), and the negative Ce anomaly is the result of the metasomatism of the mantle source.

**6. Geodynamic considerations: a back-arc basin on the Finisterra Terrane?**

The presented data suggests a crustal stretching episode during the emplacement of (ultra)mafic magmatism in the Finisterra Terrane. These amphibolites, with alkali-tholeiitic transitional features, were generated in within-plate to MORB tectonic setting, with a significant influx of incompatible elements. The tectono-magmatic environment associated with basalt genesis is not totally clear, and two hypothesis seem to be valid:

- (1) The mafic magmatism was related to the continental rifting tectonic setting, associated with mantle melting and tholeiitic within-plate to MORB magmatism, locally with transitional features. The mafic magmas were emplaced in upper crust, with assimilation of crustal components; or

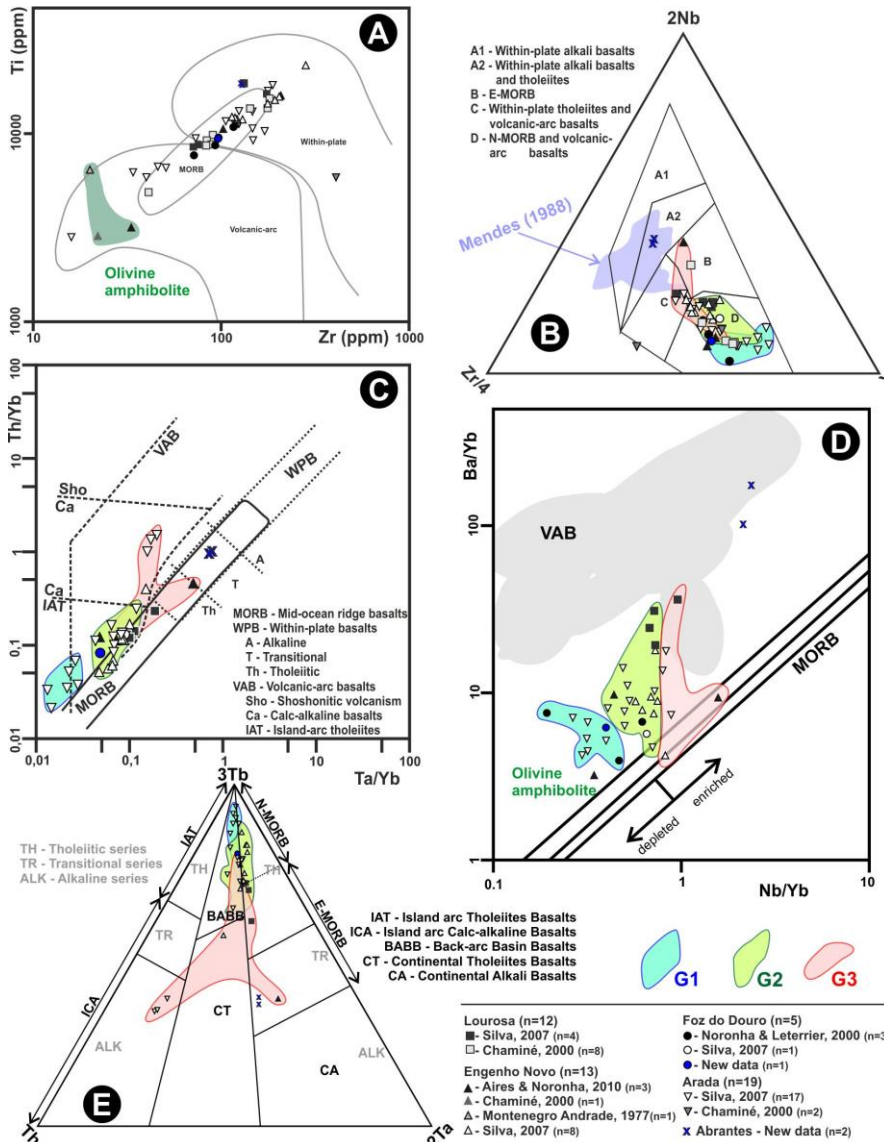


Figure 5. Tectonic discriminant diagrams used to mafic derived rocks from Finisterra Terrane: (A) Zr vs. Ti diagram (adapted from Pearce, 1982); (B) Nb-Zr-Y diagram (adapted from Meschede, 1986); (C) Ta/Yb vs. Th/Yb diagram (adapted from Pearce, 1982); (D) Nb/Yb vs. Ba/Yb diagram (adapted from Pearce and Stern, 2006); (E) Tb-Th-Ta diagram (adapted from Cabanis and Thieblemont, 1988).

Figura 5. Diagramas discriminantes para ambientes geotectónicos aplicados às rochas orto-derivadas máficas do Terreno Finisterra: (A) diagrama Zr vs. Ti (adaptado de Pearce, 1982); (B) diagrama Nb-Zr-Y (adaptado de Meschede, 1986); (C) diagrama Ta/Yb vs. Th/Yb (adaptado de Pearce, 1982); (D) diagrama Nb/Yb vs. Ba/Yb (adaptado de Pearce e Stern 2006); (E) diagrama Tb-Th-Ta (adaptado de Cabanis e Thieblemont, 1988).



(2) The mafic magmatism was generated in a back-arc basin tectonic setting, developing magmas with significant influx of subduction-mobile elements. This hypothesis explains the significant input of incompatible elements (*e.g.* Ba and Th) in mafic magmatism, as well as the negative Ce anomaly. The Abrantes amphibolites can be interpreted as transitional magmatism related with the stretching processes during the back-arc basin generation, in continental arc setting.

The age of the within-plate to MORB geochemistry magmatism in Finisterra Terrane is debatable (Neoproterozoic or Silurian-Devonian; Noronha and Leterrier, 2000; Almeida *et al.*, 2014). In the Iberian Terrane similar geochemical features were obtained for the Ediacaran mafic magmatism of Cadomian volcanic arc and related back-arc basin (*e.g.* Sáchez-Lorda *et al.*, 2014; Moreira *et al.*, 2019b) and in the Early Cambrian rifting events (*e.g.* Gómez-Pugnaire *et al.* 2003, Sanchez-Garcia *et al.*, 2010; Moreira *et al.*, 2014) of Ossa-Morena Zone. If the Silurian-Devonian ages for this magmatic mafic episode is considered, or at least for part of them, there is not a correlative episode in the Iberian Terrane (Silurian bimodal volcanic rocks were only reported in the allochthonous terranes of Galiza-Trás-os-Montes Zone; *e.g.* Ribeiro *et al.*, 2013b).

The Finisterra Terrane was recently inserted in the arcuate geometry of European Variscides (Dias *et al.*, 2016), and is well correlated with León Block and Mid German Crystalline Rise (MGCR) (Moreira *et al.*, 2019a). In the MGCR, during Silurian/Early Devonian, a magmatic-arc followed by the emplacement of a back-arc basin, generated metabasites with within-plate to MORB signature (ages ranging 405-360 Ma) (Zeh and Will, 2010). Also in the León Block, mafic and ultramafic tholeiites (*e.g.* Faure *et al.* 2010), with within-plate to MORB geochemistry signature, were described, though with no available geochronological data. Thus, the within-plate to MORB magmatism from the Finisterra Terrane seems to represent a similar event of back-arc basin genesis and the arc-related magmatism could be represented by the Foz do Douro, Souto Redondo and Lourosela biotite orthogneisses (all in Lourosa Unit), with ages ranging between 450-420 Ma (Chaminé *et al.*, 1998; Sousa *et al.*, 2014); similar ages were also identified to the arc magmatism in MGCR (Zeh and Will, 2010 and references therein). The Foz do Douro biotite orthogneiss shows volcanic-arc granite type chemical affinities (Noronha and Leterrier, 2000; Sousa *et al.*, 2018), also in accordance with the present interpretation. All those within-plate to MORB metabasalts intruded the Finisterra tectono-stratigraphic successions, as dyke structures, and can be the expression of extensional processes during Early Palaeozoic (Silurian-Devonian?), related with Variscan Ocean(s) opening or a back-arc basin related with Rheic subduction. However, it is not excluded that part of the basaltic rocks could be older (Ediacaran and/or Cambrian).

To clarify these issues, it is crucial a most representative and large sampling of metabasalt rocks for whole rock geochemistry, as well as a thoroughly isotope and geochronology studies (*e.g.* Rb/Sr, Sm/Nd, U/Pb and Pb isotopes), in order to characterize the magmatic sources and constrain their model and emplacement ages, so characterizing this episode of crustal stretching.

## Acknowledgments

This work is financed by FCT national funds through ICT projects (Refs: UIDB/04683/2020). Authors acknowledge Maria dos Anjos Ribeiro and Pedro Ferreira by the constructive review of the manuscript.

## References

- Aires, S., Noronha, F. 2010. O anfibolito olivínico do Engenho Novo (Norte de Portugal) revisitado. *Actas do X Congresso Geoquímica Países de Língua Portuguesa e XVI Semana Geoquímica*, 69-77.
- Almeida, N., Egidio Silva, M., Fonseca, P. E., Bezerra, M. H., Basei, M., Chaminé, H. I., Tassinari, C. 2014. Novos dados geocronológicos do Finisterra. *Comunicações Geológicas*, **101**(I): 31-34.
- Bellot, N., Boyet, M., Doucelance, R., Bonnard, P., Savov, I. P., Plank, T., Elliott, T., 2018. Origin of negative cerium anomalies in subduction-related volcanic samples: Constraints from Ce and Nd isotopes. *Chemical Geology*, **500**: 46-63. DOI: 10.1016/j.chemgeo.2018.09.006.
- Cabanis, P. B., Thiéblemont, D., 1988. La discrimination des tholéiites continentals et des basalts arrière-arc. Proposition d'un nouveau diagramme, le triangle Th-3Tb-2Ta. *Bulletin de la Société Géologique de France*, **IV**(6): 927-935. DOI: 10.2113/gssgfbull.IV.6.927.
- Cann, J. R., 1970. Rb, Sr, Y, Zr and Nb in some ocean floor basaltic rocks. *Earth and Planetary Science Letters*, **10**: 7-11. DOI: 10.1016/0012-821X(70)90058-0.
- Chaminé, H. I. 2000. *Estratigrafia e estrutura da Faixa Metamórfica de Espinho – Albergaria-a-Velha (Zona de Ossa Morena: Implicações geodinâmicas)*. Tese de Doutoramento (não publicado), Univ. Porto, 497.
- Chaminé, H. I., Leterrier, J., Fonseca, P. E., Ribeiro, A., Lemos de Sousa, M. J. 1998. Geocronologia U/Pb em zircoes e monazites de rochas ortoderivadas do sector Espinho-Albergaria-a-Velha (Zona de Ossa Morena, NW de Portugal). Abstracts do V Congresso Nacional de Geologia. *Comunicações do Instituto Geológico e Mineiro*, **84**(1): B115-B118.
- Chaminé, H. I., Gama Pereira, L. C., Fonseca, P. E., Noronha, F., Lemos de Sousa, M. J. 2003. Tectonoestratigrafia da faixa de cisalhamento de Porto-Albergaria-a-Velha-Coimbra-Tomar, entre as Zonas Centro-Ibérica e de Ossa-Morena (Maciço Ibérico, W de Portugal). *Cadernos do Laboratorio Xeolóxico de Laxe*, **28**: 37-78.
- Dias, R., Ribeiro, A. 1993. Porto-Tomar shear zone, a major structure since the beginning of the Variscan orogeny. *Comunicações do Instituto Geológico e Mineiro*, **79**: 29-38.
- Dias, R., Ribeiro, A., Romão, J., Coke, C., Moreira, N., 2016. A review of the Arcuate Structures in the Iberian Variscides; Constraints and Genetic Models. *Tectonophysics*, **681C**: 170-194. DOI: 10.1016/j.tecto.2016.04.011.
- Díez Fernández, R., Pereira, M. F., 2017. Strike-slip shear zones of the Iberian Massif: Are they coeval? *Lithosphere*, **9**(5): 726-744. DOI: 10.1130/L648.1.
- Faure, M., Sommers, C., Melleton, J., Cocherie, A., Lautout, O. 2010. The Léon domain (French Massif armoricain): a westward extension of the Mid-German Crystalline Rise? Structural and geochronological insights. *International Journal of Earth Sciences*, **99**: 65-81. DOI: 10.1007/s00531-008-0360-x.
- Ferreira Soares, A. F., Marques, J., Sequeira, A. 2007. *Notícia Explicativa da Folha 19-D Coimbra-Lousã da Carta Geológica de Portugal, na escala 1:50 000*, LNEG, 71.
- German, C. R., Elderfield, H., 1990. Application of the Ce anomaly as a paleoredox indicator: the ground rules. *Paleoceanography*, **5**(5): 823-833. DOI: 10.1029/PA005i005p00823.
- Gómez-Pugnaire, M., Azor, A., Fernández-Soler, J., Sánchez-Vizcaíno V. L., 2003. The amphibolites from the Ossa-Morena/Central Iberian Variscan suture (Southwestern Iberian Massif): Geochemistry and tectonic interpretation. *Lithos*, **68**: 23-42. DOI: 10.1016/S0024-4937(03)00018-5.
- Gutiérrez-Alonso, G., Collins, A. S., Fernández-Suárez, J., Pastor-Galán, D., González-Clavijo, E., Jourdan, F., Weil, A. B., Johnston, S. T., 2015. Dating of lithospheric buckling: <sup>40</sup>Ar/<sup>39</sup>Ar ages of syn-orocline strike-slip shear zones in northwestern Iberia. *Tectonophysics*, **643**: 44-54. DOI: 10.1016/j.tecto.2014.12.009.
- Hole, M., Saunders, A., Marriner, G., Tarney, J., 1984. Subduction of Pelagic Sediments - Implications for the origin of Ce-Anomalous Basalts from the Mariana Islands. *Journal of the Geological Society*, **141**: 453-472. DOI: 10.1144/gsjgs.141.3.0453.
- Irvine, T. N., Baragar, W. R. A. 1971. A guide to the chemical

- classification of the common volcanic rocks. *Canadian Journal of Earth Sciences*, **8**: 523-548. DOI: 10.1139/e71-055.
- Kelemen, P. B., Hanghøj, K., Greene, A. R., 2014. One view of the Geochemistry of Subduction-Related Magmatic Arcs, with an Emphasis on Primitive Andesite and Lower Crust. In: Holland, H. D., Turekian K. K. (Eds.), *Treatise on geochemistry: The Crust*, Elsevier, **4**: 123-146. DOI: 10.1016/B978-0-08-095975-7.00323-5.
- Le Maitre, R. W., Bateman, P., Dudek, A., Keller, J. et al., 1989. *A Classification of Igneous rocks and Glossary of Term: Recommendations of the International Union of Geological Sciences Subcommittee on the Systematics of Igneous Rocks*. Blackwell Scientific Publications, Oxford, 193.
- Machado, G., Francu, E., Vavrdová, M., Flores, D., Fonseca, P. E., Rocha, F., Gama Pereira, L. C., Gomes, A., Fonseca, M., Chaminé, H.I. 2011. Stratigraphy, palynology and organic geochemistry of the Devonian-Mississippian metasedimentary Albergaria-a-Velha Unit (Porto-Tomar Shear Zone, W Portugal). *Geological Quarterly*, **55**(2): 139-164.
- Mendes, M. H. A. H., 1988. *Contribuição para o estudo das rochas metamórficas aflorantes entre Ovar e Espinho*. Tese de Mestrado (não publicada), Univ. Aveiro, 186.
- Meschede, M., 1986. A method of discriminating between different types of mid-ocean ridge basalts and continental tholeiites with the Nb-Zr-Y diagram. *Chemical Geology*, **56**(3-4): 207-218. DOI: 10.1016/0009-2541(86)90004-5.
- Montenegro de Andrade, M., 1977. O Anfibólito olivínico do Engenho Novo (Vila da Feira). *Comunicações dos Serviços Geológicos de Portugal*, **61**: 43-61.
- Moreira, N., 2017. *Evolução Geodinâmica dos sectores setentrionais da Zona de Ossa-Morena no contexto do Varisco Ibérico*. Tese de Doutoramento (não publicado), Univ. Évora, 433.
- Moreira, N., Araújo, A., Pedro, J. C., Dias, R., 2014. Geodynamic evolution of Ossa-Morena Zone in SW Iberian context during the Variscan Cycle. *Comunicações Geológicas*, **101**(I): 275-278.
- Moreira, N., Romão, J., Pedro, J., Dias, R., Ribeiro, A., 2016. The Porto-Tomar-Ferreira do Alentejo Shear Zone tectonostratigraphy in Tomar-Abrantes sector (Portugal). IX Congreso Geológico de España. *Geo-Temas* (volume especial), **16**(1): 85-88.
- Moreira, N., Romão, J., Dias, R., Ribeiro, A., Pedro, J., 2019a. The Finisterra-Léon-Mid German Crystalline Rise Domains; proposal of a new terrane in the Variscan Chain. In: Quesada, C., Oliveira, J. T. (Eds.), *The Geology of Iberia: a geodynamic approach* (Vol. 2). Springer (Berlin), Regional Geology Review series, 207-228. DOI: 10.1007/978-3-030-10519-8\_7.
- Moreira, N., Pedro, J., Romão, J., Dias, R., Ribeiro, A., 2019b. The Neoproterozoic magmatism in NW of the Ossa-Morena Zone (Abrantes, Portugal): new insights of Cadomian magmatic arc? *Actas do XII Congresso Ibérico de Geoquímica | XX Semana da Geoquímica* (Évora), 157-160.
- Neal, C.R., Taylor, L. A., 1989. A negative Ce anomaly in a periodotite xenolith: evidence for crustal recycling into the mantle or mantle metasomatism? *Geochimica et Cosmochimica Acta*, **53**: 1035-1040. DOI: 10.1016/0016-7037(89)90208-1.
- Noronha, F., Leterrier, J., 2000. Complexo Metamórfico da Foz do Douro (Porto). *Geoquímica e Geocronologia. Revista Real Academia Galega de Ciências*, **XIV**: 21-42.
- Pearce, J. A., 1982. Trace element characteristics of lavas from destructive plate boundaries. In: Thorpe, R. S. (Ed.), *Andesites*. New York, John Wiley & Sons, 525-548.
- Pearce, J. A., 2014. Immobile element fingerprinting of ophiolites. *Elements*, **10**(2): 101-108. DOI: 10.2113/gselements.10.2.101.
- Pearce, J. A., Cann, J. R., 1973. Tectonic setting of basic volcanic rocks determined using trace element analyses. *Earth and Planetary Science Letters*, **19**(2): 290-300. DOI: 10.1016/0012-821X(73)90129-5.
- Pearce, J. A., Stern, R. J., 2006. Origin of Back-Arc Basin Magmas: Trace Element and Isotope Perspectives. *Geophysical Monograph Series*, **166**: 63-86. DOI: 10.1029/166GM06.
- Pereira, M. F., Silva, J. B., Drost, K., Chichorro, M., Apraiz, A., 2010. Relative timing of the transcurrent displacements in northern Gondwana: U-Pb laser ablation ICP-MS zircon and monazite geochronology of gneisses and sheared granites from the western Iberian Massif (Portugal). *Gondwana Research*, **17**(2-3): 461-481. DOI: 10.1016/j.gr.2009.08.006.
- Ribeiro, A., Munhá, J., Dias, R., Mateus, A., Pereira, E., Ribeiro, L., Fonseca, P. E., Araújo, A., Oliveira, J. T., Romão, J., Chaminé, H. I., Coke, C., Pedro, J. C., 2007. Geodynamic evolution of the SW Europe Variscides. *Tectonics*, **26**(6): TC6009. DOI: 10.1029/2006tc002058.
- Ribeiro, A., Romão, J., Munhá, J., Rodrigues, J., Pereira, E., Mateus, A., Araújo, A., 2013a. Relações tectonostratigráficas e fronteiras entre a Zona Centro-Ibérica e a Zona Ossa-Morena do Terreno Ibérico e do Terreno Finisterra. In: Dias, R., Araújo, A., Terrinha, P., Kullberg, J. C. (Eds.), *Geologia de Portugal*, Escolar Editora, **1**: 439-481.
- Ribeiro, A., Pereira, E., Ribeiro, M. L., Castro, P., 2013b. Unidades alóctones da região de Morais (Trás-os-Montes oriental). In: Dias, R., Araújo, A., Terrinha, P., Kullberg, J. C. (Eds.), *Geologia de Portugal*, Escolar Editora, **1**: 333-376.
- Ribeiro, M. A., Areias, M., Ferreira, J., Martins, H., Sant'Ovaia, H., 2015. Geological and petrological constraints on the variscan evolution of the NW area of Port-Viseu Belt. *Géologie de la France* (special issue), Rennes, **2015**(1): 119-120.
- Ribeiro, M. A., Martins, H., Sant'Ovaia, H., Dória, A., 2016. Late-variscan ductile-brittle deformation in central Iberian autochthon (NW Portugal): Tectonic implications. *International Multidisciplinary Scientific GeoConference Surveying Geology and Mining Ecology Management*, SGEM2016, **1**: 313-320.
- Romão, J., Moreira, N., Pedro, J. C., Mateus, A., Dias, R., Ribeiro, A., 2013. Contribuição para o conhecimento das unidades tectonostratigráficas do Terreno Finisterra na região de Tomar. In: Moreira, N., et al. (Eds.), *Geodinâmica e Tectónica Global; a Importância da Cartografia Geológica*, 9ª Conferência GGET-SGP, Estremoz, 87-91.
- Romão, J., Moreira, N., Dias, R., Pedro, J., Mateus, A., Ribeiro, A., 2014. Tectonostratigrafia do Terreno Ibérico no sector Tomar-Sardoal-Ferreira do Zêzere e relações com o Terreno Finisterra. *Comunicações Geológicas*, **101**(I): 559-562.
- Sánchez-García, T., Bellido, F., Pereira, M. F., Chichorro, M., Quesada, C., Pin, C., Silva, J. B., 2010. Rift-related volcanism predating the birth of the Rheic Ocean (Ossa-Morena zone, SW Iberia). *Gondwana Research*, **17**(2): 392-407. DOI: 10.1016/j.gr.2009.10.005.
- Sanchez-Lorda, M. E., Sarrionandia, F., Ábalos, B., Carracedo, M., Eguíluz, L., Gil Ibarguchi, J. I., 2014. Geochemistry and paleotectonic setting of Ediacaran metabasites from the Ossa-Morena Zone (SW Iberia). *International Journal of Earth Sciences*, **103**: 1263-1286. DOI: 10.1007/s00531-013-0937-x.
- Shervais, J. W., 1982. Ti-V plots and the petrogenesis of modem and ophiolitic lavas. *Earth and Planetary Science Letters*, **59**: 101-118. DOI: 10.1016/0012-821X(82)90120-0.
- Shimizu, H., Sawatari, H., Kawata, Y., Dunkley, P. N., Masuda, A., 1992. Ce and Nd isotope geochemistry on island arc volcanic rocks with negative Ce anomaly: existence of sources with concave REE patterns in the mantle beneath the Solomon and Bonin island arcs. *Contributions to Mineralogy and Petrology*, **110**: 242-252. DOI: 10.1007/BF00310741.
- Silva, S., 2007. *Estudo geoquímico de metabasitos da ZOM e da ZCI aflorantes na região Centro-Norte de Portugal*. Tese de Mestrado (não publicado), Univ. Aveiro, 180.
- Sousa, M., Sant'Ovaia, H., Tassinari, C., Noronha, F., 2014. Geocronologia U-Pb (SHRIMP) e Sm-Nd do ortogneisse biotítico do Complexo Metamórfico da Foz do Douro (NW de Portugal). *Comunicações Geológicas*, **101**(I): 225-228.
- Sousa, M., Sant'Ovaia, H., Noronha, F., 2018. Geoquímica dos ortogneisses do "Complexo Metamórfico da Foz do Douro. *Actas do XIV Congresso de Geoquímica dos Países de Língua Portuguesa e XIX Semana de Geoquímica*, Vila Real, 107-110.
- Sun, S. S., McDonough, W. F., 1989. Chemical and isotopic systematics of oceanic basalts: implications for mantle composition and processes. In: Saunders, A. D., Norry, M. J. (Eds.), *Magmatism in the Ocean Basins*, Geological Society London Special Publication, **42**: 313-345.
- Vermeesch, P., 2006. Tectonic discrimination diagrams revisited. *G3 Geochemistry, Geophysics, Geosystems*, **7**: Q06017. DOI: 10.1029/2005GC001092.
- Zeh, A., Will, T. M., 2010. The Mid-German Crystalline Rise. In: Linnemann, U., Romer, R. L. (Eds.), *Pre-Mesozoic geology of Saxo-Thuringia—From the Cadomian active margin to the Variscan orogen*. Schweizerbart, Stuttgart, 195-220.